UNIVERSITÄT GREIFSWALD
Wissen lockt. Seit 1456

Faculty of Mathematics and Natural Sciences

Photon Dynamics in Curved Spacetimes

Bachelor's Thesis

Christoph Gärtner

Greifswald, August 12, 2018

Supervisor and First Reviewer
Prof. Dr. Ralf Schneider

Second Reviewer
Prof. Dr. Lutz Schweikhard

Contents

1 Introduction

Starting out, the motivation for this thesis was investigation of relativistic frequency shifts in Kerr-de Sitter spacetime, which models charge neutral stationary rotating black holes embedded in a universe with non-vanishing cosmological constant. This particular spacetime was chosen because its metric is sufficiently complex to make numeric simulation attractive, and it is relevant in practice. The initial hope was to obtain results pertaining to unique phenomenology or with direct applicability to actual observation.

This hope has not quite been fulfilled. Instead, what will be presented are preliminary results that should be understood as stepping stones towards this goal. This includes a description of the physics of relativistic frequency shift, a derivation of one version of the Kerr-de Sitter metric, and some calculations performed in various limits of the full Kerr-de Sitter spacetime. Some shortcomings of the current approach will be described and possible ways to improve upon it will be mentioned.

1.1 Physical Background

The theory of General Relativity describes gravity as a consequence of spacetime curvature, affecting massive and massless test particles alike. In a sense, it is still true that in absence of additional forces, particles continue to move along straight lines. However, the meaning of *straight* has to be adjusted once we look beyond the pseudo-Euclidean geometry of flat Minkowski spacetime.

In addition to the effect of curvature on particle trajectories, there is a secondary effect, in case of photons manifesting as a shift in frequency when comparing measurements performed at the source to those made by distant observers. Phenomenologically, this effect is described in a number ways: In case of relative motion in weak gravitational fields, it is recognized as special relativistic Doppler shift, presented as a generalization of ordinary Doppler shift of classical waves in a medium. At large distances, cosmological redshift can be observed, a change in wave length of an electromagnetic wave due to the metric expansion of space itself. Near large masses, it is described as gravitational redshift, explained by a loss of energy when climbing out of the potential well, or as a consequence of gravitational time dilation.

In this thesis, unified descriptions of all of these effects will be presented, one of them dynamic in terms of timings of consecutive wave fronts, the other kinematic in terms of parallel transport of photon momentum. The discussion will be restricted to massless particles, though similar effects can be observed with massive particles as well, where they manifest as a loss of kinetic energy instead of a shift in frequency.[1]

[1] One could make an analogy between the de Broglie waves of massive particles and electromagnetic

1.2 Outline of this Thesis

Following this introduction, the second part of this thesis will very briefly recapitulate some relevantconcepts from Riemannian geometry and General Relativity. The third part presents the unified descriptions of relativistic frequency shifts. The fourth part investigates exemplary spacetimes, recovering the phenomenology. The fifth part introduces the Kerr-de Sitter spacetime via the Kerr-Schild ansatz. The sixth part describes the methodology of the numeric simulation. The seventh part will present the results obtained from simulating photon dynamics in various limiting cases of Kerr-de Sitter spacetime. In the final part, results will be summarized and put into context.

waves, for example arguing that cosmological redshift due to spatial expansion should therefore affect massive particles as well. Speaking from personal experience, this argument is rarely made.

2 A Brief Review of Geometry and Relativity

The theory of General Relativity is based on concepts from Riemannian geometry, with the twist that it deals with a metric tensor of Lorentzian instead of Euclidean signature. A comprehensive introduction to either subject is beyond the scope of this thesis, and familiarity with basic concepts from differential geometry such as differentiable manifolds, coordinate maps, tangent vectors and covectors, tensors, the physical meaning of the metric tensor or the distinction between space-like, time-like or light-like vectors will be assumed.

Nevertheless, this section will review certain aspects of General Relativity that are relevant to the subject at hand.

2.1 Notational Conventions

The bases of tangent and cotangent space induced by a coordinate map x^μ will be denoted by ∂_μ and $\mathrm{d}\, x^\mu$ respectively. When convenient, vectors $\mathbf{v} = v^\mu \partial_\mu$ and covectors $\mathbf{P} = p_\mu \,\mathrm{d}\, x^\mu$ will be referred to as v^μ and p_μ in keeping with physicists' conventions.

Metric tensors will be written as

$$\mathrm{d}\, s^2 = g_{\mu\nu} \,\mathrm{d}\, x^\mu \,\mathrm{d}\, x^\nu$$

in terms of symmetrized tensor products

$$\mathrm{d}\, x^\mu \,\mathrm{d}\, x^\nu = \frac{1}{2}(\mathrm{d}\, x^\mu \otimes \mathrm{d}\, x^\nu + \mathrm{d}\, x^\nu \otimes \mathrm{d}\, x^\mu)$$

and will have signature $(-+++)$.

The Einstein convention of summation over repeated tensor indices has been adopted as well as implicit raising and lowering of indices by contraction with the metric tensor.

2.2 Levi-Civita Connection

Spacetime is modelled as a pseudo-Riemannian differential manifold, a smooth real space with geometric and topological structure, locally described via coordinate maps into $\mathbb{R}^4$. Its geometric structure is given by the metric tensor, a fiber-wise product on the tangent bundle, which consists of linear vector spaces attached to any base point of the manifold.

A priori, the spaces tangent to different points should be considered independent, and additional structure is needed to relate vectors rooted in distinct points. This structure is the affine connection, which can be understood geometrically as a horizontal subbundle of the double tangent bundle [11, ch. 9]. In general, it relates vectors

only at infinitesimal distances, and if a finite change is built up by integrating infinitesimal changes along a path, the result will in general be path-dependent. This failure of distance parallelism is measured by curvature, an obstruction against integrability of the horizontal subbundle. In case of metric connections specifically, it is also an obstruction against isometries into (pseudo-)Euclidean space.

Connections that are compatible with the metric may differ in torsion, a freedom to twist orthogonal frames while moving along a curve. There is however a unique torsion-free connection compatible with the metric, the Levi-Civita Connection.

In terms of the metric $g_{\mu\nu}$, its connection coefficients are the Christoffel symbols [11, ch. 29]

$$\Gamma^{\lambda}{}_{\mu\nu} = \frac{1}{2} g^{\lambda\alpha} \left(\partial_\nu g_{\alpha\mu} + \partial_\mu g_{\alpha\nu} - \partial_\alpha g_{\mu\nu} \right) .$$

This is the connection used in General Relativity.

2.3 Einstein Field Equations

To venture beyond mathematics into the realm of physics, it is important to know which metric (and thus which connection) correspond to a given physical situation. This goal is achieved by the Einstein field equation [4][12, ch. 17]

$$R_{\mu\nu} - \frac{1}{2} R g_{\mu\nu} + \Lambda g_{\mu\nu} = \frac{8\pi G}{c^4} T_{\mu\nu} \,,$$

relating geometric objects on the left-hand side to the matter distribution on the right-hand side. It can be derived from the Einstein-Hilbert action [8][12, ch. 21]

$$S = \int \left(\frac{c^4}{16\pi G} (R - 2\Lambda) + \mathcal{L}_M \right) \sqrt{-g} \, \mathrm{d}^4 \, x$$

Here, $R_{\mu\nu}$ denotes the Ricci curvature tensor, R the scalar curvature, $g_{\mu\nu}$ the metric tensor and g its determinant, Λ a cosmological constant and G and c are the gravitational constant and the speed of light. $R_{\mu\nu}$ and R are obtained from the Riemann curvature tensor by contraction.[2]

The source of gravity is the stress-energy-momentum tensor $T_{\mu\nu}$ derived from the matter lagrangian $\mathcal{L}_M$.[3] However, this thesis is mainly concerned with vacuum solutions $T_{\mu\nu} = 0$ and in particular black hole solutions.[4]

In this thesis, the Einstein equation will be needed once when the Kerr-Schild approach to finding new metrics will be discussed, but they won't be solved explicitly.

[2] in ordinary Riemannian geometry, the Ricci tensor carries information about the directional change in volume compared to flat space and the spread of geodesics, though the situation is less intuitive in case of Lorentzian signature of the metric

[3] technically the Belinfante–Rosenfeld tensor as potential asymmetry of the canonical tensor needs to be accounted for

[4] black holes count as vacuum solutions as energy-momentum vanishes everywhere except for the singularities, which need to be removed from the manifold

2.4 Parallel Transport

Once a manifold has been equipped with a connection, any curve γ within the manifold will induce isomorphisms $\Gamma(\gamma)_{t_0}^{t}$ between any two tangent spaces along γ. Here, t_0 and t are values of the curve parameter.

Connections where these isomorphisms are isometries are called metric, with the Levi-Civita connection the prime example.

This means that a vector $\mathbf{v}_0$ chosen at a single point visited by the curve will give rise to a vector field $\mathbf{v}(t) = \Gamma(\gamma)_{t_0}^{t}\mathbf{v}_0$ along γ. In terms of the local expression $x^\mu(t)$ of γ, this is the parallel transport equation

$$\frac{\mathrm{d}\, v^\mu}{\mathrm{d}\, t} + \Gamma^\mu{}_{\alpha\beta}\frac{\mathrm{d}\, x^\alpha}{\mathrm{d}\, t}v^\beta = 0 \tag{1}$$

Parallel transport will play a central role in the upcoming discussion of relativistic frequency shifts.

2.5 Autoparallels

Autoparallels are the answer to the question *What's a straight line in a curved space?* A straight line is a curve with unchanging direction. The ability to compare directions (represented by tangent vectors obtained from differentiating by a curve parameter) is made possible by a connection. The local expression

$$\frac{\mathrm{d}^2 x^\mu}{\mathrm{d}\lambda^2} + \Gamma^\mu{}_{\alpha\beta}\frac{\mathrm{d}x^\alpha}{\mathrm{d}\lambda}\frac{\mathrm{d}x^\beta}{\mathrm{d}\lambda} = 0 \tag{2}$$

is known as the geodesic equation.[5] In light of the parallel transport equation (1), it states that a velocity vector of a geodesic gets transported into the velocity vector at the destination. Solving the above equation does not merely fix a curve, but also its parametrization, which will be unique up to affine transformations and in particular constant rescalings. Eigentime is such a parameter, made unique[6] by a normalization condition on the tangent vectors known as fourvelocities.

From the perspective of physics, moving along unchangingly is the most obvious generalization of the concept of force-free motion. From this perspective, gravitationally induced acceleration is merely the test particle maintaining its state of motion according to the first of Newton's laws.

The geodesic equation (2) is the equation of motion that is going to be integrated numerically when pushing particles through spacetime.

[5] however, geodesics in the sense of distance-minimizing curves and autoparallels do not agree in the presence of torsion

[6] up to a constant offset

3 Unifying Descriptions of Frequency Shifts

In this section, two generic approaches for computing relativistic frequency shifts will be introduced. Note that a complete (classical) description of propagation of light in curved spacetimes will not be developed: In full generality, this would require solving the Einstein-Maxwell system of coupled non-linear differential equations, a task beyond the scope of this work. Instead, it is assumed that the energy-momentum of the light wave is negligible and does not contribute to the dynamic of the metric.

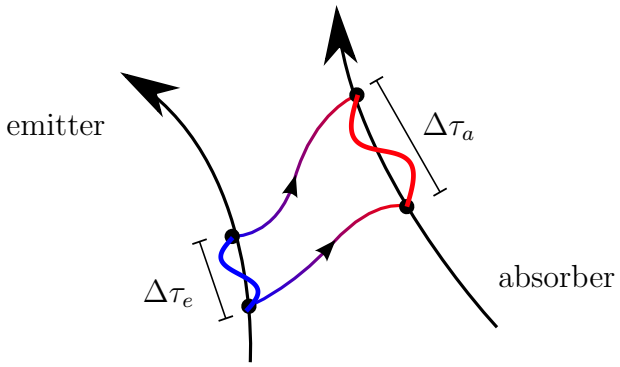

Figure 1: Two consecutive wave fronts travelling along light rays (coloured), intersecting with the world lines of emitter and absorber (black)

3.1 Frequency Shift from Wave Front Timings

Assuming the validity of the limit of geometrical optics, a light ray in vacuum will trace out a null geodesic. The path taken will be affected by nearby sources of gravity, and measurement of deflection of starlight passing the sun was an important historical milestone[7] for the fledgling theory of General Relativity [16].

In this model, relativistic frequency shifts can be obtained by comparing the (proper) time interval between the emission of consecutive wavefronts at the source and the time interval between their absorption as measured by a distant observer.

Expressing the redshift $z = \frac{\lambda_a - \lambda_e}{\lambda_e}$ in terms of frequencies ν and periods $\Delta\tau = \nu^{-1}$ instead of wavelengths λ, it is given by

$$1 + z = \frac{\lambda_a}{\lambda_e} = \frac{\nu_e}{\nu_a} = \frac{\Delta\tau_a}{\Delta\tau_e} \tag{3}$$

where the indices denote emitter (e) and absorber (a). Figure 1 depicts this idea.

While this approach is intuitively appealing and can be very convenient when analysing static situations, it has a number of shortcomings, which will be dealt with in the next section.

[7] while the effect had already been predicted from Newtonian gravity, derivation of the observed angle of deflection requires a relativistic calculation

3.2 Frequency Shift from Momentum Transport

Above, measurements over finite time intervals were used to determine the frequency shift. This will yield an integrated effect that depends on the intermediate motion of emitter and absorber and the background dynamics of the spacetime. Also note that the freedom to choose other timing intervals besides full periods exist, and the result will in general depend on this arbitrary choice. In principle, wave packets consisting of a large number of frequencies also have to be dealt with somehow.

More pragmatically, from a computational perspective, the less moving parts one has to track, the better. So letting the timing interval go to zero, one needs an infinitesimal description of the wave. The physical quantity that does this is the wave (co-)vector[8] k_μ, describing the wave's spatio-temporal periodicity. It's time-like component is the wave's angular frequency, which can be extracted by contraction with the fourvelocity u^μ of the observer in question,

$$\omega_{\text{observed}} = k_\mu u^\mu \ .$$

The redshift will then be given by

$$1 + z = \frac{\omega_e}{\omega_a} = \frac{k_\nu(t_e)\, v^\nu(t_e)}{k_\mu(t_a)\, u^\mu(t_a)} \tag{4}$$

where v^ν is the fourvelocity of the source and we have parametrized the vector fields k_μ, u^μ, v^μ (which in general are only defined along the corresponding worldlines) by coordinate time for notational convenience.

Now, according to de Broglie's relation, wave and momentum covectors are related by

$$p_\mu = \hbar k_\mu$$

and (4) can be recast as

$$1 + z = \frac{E_e}{E_a} = \frac{p_\nu(t_e)\, v^\nu(t_e)}{p_\mu(t_a)\, u^\mu(t_a)} \tag{5}$$

in terms of photon energies E.

Furthermore, if the photon trajectory $\gamma = x^\mu(\lambda)$ is parameterized by an affine parameter λ,[9] the momentum *vector* will be proportional to the curve's tangent vector respective λ, that is

$$p^\mu(t) = \epsilon\, \dot{x}^\mu(\lambda(t))$$

for some constant of proportionality ϵ and at all times t, and thus

$$1 + z = \frac{g_{\mu\nu}(t_e)\, \dot{x}^\mu(\lambda(t_e))\, v^\nu(t_e)}{g_{\alpha\beta}(t_a)\, \dot{x}^\alpha(\lambda(t_a))\, u^\beta(t_a)} \ . \tag{6}$$

[8] in dispersive media, the energy-momentum tensor might not be symmetric, and we would have to distinguish between momentum density and energy flux, or, respectively, wave and Poynting vector; this possibility will be ignored

[9] this is automatic if the trajectory has been obtained by solving the geodesic equation

If γ is not affinely parameterized, that proportionality won't hold, and one needs to explicitly compute

$$\mathbf{p}(t_a) = \Gamma(\gamma)^{\lambda(t_a)}_{\lambda(t_e)} \cdot \mathbf{p}(t_e)\,,$$

that is, solve (1) for p^μ in place of the generic v^μ.

Finally, how should this result be interpreted? It shows that relativistic frequency shifts can be understood kinematically, an interpretation that works for massless and massive particles alike: Kinetic energy is a frame-dependent quantity, and in curved spacetimes lacking distance parallelism, the relative change between the orientation of particle momentum and velocities of source and observer at the moment of emission and absorption, which is what determines the observed shift in energy, will depend on the path that was taken through spacetime. From this perspective, there is no difference between photons getting their frequencies shifted, and massive particles losing or picking up speed while travelling through gravitational fields.

3.3 Frequency Shift and Conservation of Canonical Energy

The procedure above can be notably simplified if the metric is independent of the time coordinate, and source and observer are sitting still at fixed spatial coordinates.

The starting point is a 'dynamic Lagrangian' $L = L(x^\mu, \dot{x}^\nu)$ given by [12, ch. 13]

$$L = \frac{1}{2} g_{\mu\nu} \dot{x}^\mu \dot{x}^\nu\,,$$

which has the geodesic equation as Euler-Lagrange equations.

The canonical momenta are given by

$$\pi_\mu = \frac{\partial L}{\partial x^\mu} = g_{\mu\nu}\dot{x}^\nu$$

where the letter π has been chosen to show that this is not physical momentum.

If the metric has no dependence on a particular coordinate, then the corresponding component of π_μ will be conserved. In particular, if there is no explicit time dependence, we have

$$\pi_0 = \text{const}\,.$$

Now, the fourvelocity vectors for source and observer sitting at fixed spatial coordinates are proportional to ∂_0, but have to be normalized, yielding

$$v^\mu \partial_\mu = \frac{1}{\sqrt{-g_{00}}}\partial_0 \qquad\qquad u^\mu \partial_\mu = \frac{1}{\sqrt{-g_{00}}}\partial_0\,.$$

Putting things together, (6) simplifies to

$$1 + z = \frac{\pi_0(t_e)\,\frac{1}{\sqrt{-g_{00}(t_e)}}}{\pi_0(t_a)\,\frac{1}{\sqrt{-g_{00}(t_a)}}} = \frac{\sqrt{-g_{00}(t_a)}}{\sqrt{-g_{00}(t_e)}}\,. \tag{7}$$

This concludes the discussion of frequency shift as a kinematic effect.

4 Exemplary Spacetimes

A number of toy models showcasing the phenomenology will be presented in the following section before moving on to the other main topic of this thesis.

4.1 Minkowski Spacetime and Relativistic Doppler Effect

Minkowski spacetime is flat, and inertial frames that make the connection coefficients vanish exist even globally. In such a frame, parallel transport becomes trivial. The problem will be further simplified by restriction to two dimensions and the assumption that the inertial laboratory frame is comoving with the observer.

Let the metric be given by

$$\mathrm{d}\,s^2 = -c^2\,\mathrm{d}\,t^2 + \mathrm{d}\,x^2$$

and the observer velocity at time of absorption by

$$u^\mu \partial_\mu = \partial_t\,.$$

At time of emission, let the source move away with velocity

$$v^\mu \partial_\mu = \gamma(\partial_t + v\partial_x) \qquad\qquad \gamma = \frac{1}{\sqrt{1-\left(\frac{v}{c}\right)^2}}\,.$$

The photon will travel in a straight line from source to observer. Let its momentum at time of emission be

$$p_\mu\,\mathrm{d}\,x^\mu = \frac{E}{c}(-c\,\mathrm{d}\,t - \mathrm{d}\,x)\,.$$

As the parallel transport is trivial, we have $p_\mu(t_a) = p_\mu(t_e) = p_\mu$, yielding a redshift

$$1 + z = \frac{p_\nu v^\nu}{p_\mu u^\mu} = \frac{\gamma\frac{E}{c}(-c-v)}{-\frac{E}{c}c} = \frac{1+\frac{v}{c}}{\sqrt{1-\left(\frac{v}{c}\right)^2}} = \sqrt{\frac{c+v}{c-v}}\,.$$

The more common phenomenological derivation proceeds along the lines of wavefront timings discussed in section 3.1.

4.2 FLRW Spacetime and Cosmological Redshift

A spatially homogeneous and isotropic universe can be described in terms of the FLRW[10] metric. Choosing reduced-circumference polar coordinates, it is given by [3, ch. 22.7]

$$\mathrm{d}\,s^2 = -c^2\,\mathrm{d}\,t^2 + a^2(t)\left[\frac{1}{1-k(r/r_0)^2}\,\mathrm{d}\,r^2 + r^2\,\mathrm{d}\,\Omega^2\right]$$

[10] after Alexander Friedmann, Georges Lemaître, Howard P. Robertson and Arthur Geoffrey Walker

in terms of cosmological time t, comoving radial distance r, a dimensionless scale factor $a(t)$, a characteristic length r_0 and a curvature parameter $k = -1, 0, +1$ respectively representing hyperbolic, Euclidean and elliptical spatial geometry. The element of solid angle is given by $\mathrm{d}\,\Omega^2 = \mathrm{d}\,\vartheta^2 + \sin^2\vartheta\,\mathrm{d}\,\varphi^2$.

In terms of the radius of curvature[11] $R = r_0\,a$ and dimensionless conformal coordinates η, χ implicitly defined by $c\,\mathrm{d}\,t = R(\eta)\,\mathrm{d}\,\eta$ and $r(\chi) = r_0\,\Sigma(\chi)$ where

$$\Sigma(\chi) = \begin{cases} \sinh\chi & \text{for } k = -1 \\ \chi & \text{for } k = 0 \\ \sin\chi & \text{for } k = +1 \end{cases},$$

this can be recast[12] as [12, p. 731]

$$\mathrm{d}\,s^2 = R^2(\eta)\left[-\mathrm{d}\,\eta^2 + \mathrm{d}\,\chi^2 + \Sigma^2(\chi)\,\mathrm{d}\,\Omega^2\right].$$

Cosmological redshift can be derived from parallel transport along null geodesics. By rotational symmetry, purely radial solutions to the equations of motion exist, in which case the problem reduces to two dimensions, yielding an effective metric

$$\mathrm{d}\,s^2 = R^2(\eta)\left[-\mathrm{d}\,\eta^2 + \mathrm{d}\,\chi^2\right]. \tag{8}$$

Parallel transport does not depend on affine parametrization of the curve. Choosing η as curve parameter, the trajectory is defined in terms of the dependence $\chi = \chi(\eta)$.

The tangent vector q^μ is then

$$q^\mu\partial_\mu = \partial_\eta + \frac{\mathrm{d}\,\chi}{\mathrm{d}\,\eta}\partial_\chi$$

with square

$$q_\mu q^\mu = R^2\left(-1 + \left(\frac{\mathrm{d}\,\chi}{\mathrm{d}\,\eta}\right)^2\right).$$

In case of photons, the square needs to vanish, ie

$$\frac{\mathrm{d}\,\chi}{\mathrm{d}\,\eta} = \pm 1\,,$$

fixing everything up to sign. The ingoing solution

$$q^\mu\partial_\mu = \partial_\eta - \partial_\chi$$

will be discussed.

[11] in the Euclidean case $k = 0$, it does not describe curvature, but is an arbitrary length scale

[12] assuming the implicit definitions, verification boils down to checking that $r_0^2\,\mathrm{d}\,\chi^2 = 1/\left(1 - k(r/r_0)^2\right)\mathrm{d}\,r^2$

Let a distant source emit a photon at time η_e, getting absorbed by an observer sitting at the origin of our coordinate system at time η_a. Let furthermore emitter and absorber be at rest relative to the Hubble flow, i.e. at rest relative to a comoving spatial coordinate like χ.

Their velocity vectors at time of emission and absorption will then be given by[13]

$$u^\mu(t_a)\,\partial_\mu = \frac{c}{R_a}\partial_\eta \qquad\qquad v^\mu(t_e)\,\partial_\mu = \frac{c}{R_e}\partial_\eta$$

where $R_a = R(\eta_a), R_e = R(\eta_e)$.

To parallel transport the momentum vector p^μ, note that it remains null, i.e.

$$p^\mu(\eta)\partial_\mu = \epsilon(\eta)(\partial_\eta - \partial_\chi)$$

for some function ϵ. It is therefore enough to look at just one component of p^μ.

Choosing the time component, the following Christoffel symbols[14] are required for the calculation:

$$\Gamma^\eta{}_{\eta\eta} = \Gamma^\eta{}_{\chi\chi} = \frac{\dot{R}}{R} \qquad\qquad \Gamma^\eta{}_{\eta\chi} = \Gamma^\eta{}_{\chi\eta} = 0$$

Here, the dot denotes differentiation by η.

Plugging into the parallel transport equation (1) yields

$$\dot{\epsilon} + 2\frac{\dot{R}}{R}\epsilon = 0\,.$$

Dividing by ϵ, this implies

$$0 = \frac{\mathrm{d}}{\mathrm{d}\,\eta}\ln\epsilon + 2\frac{\mathrm{d}}{\mathrm{d}\,\eta}\ln R = \frac{\mathrm{d}}{\mathrm{d}\,\eta}\ln \epsilon R^2$$

which in turn implies

$$\epsilon R^2 = \mathrm{const}\,.$$

and in particular

$$\epsilon_a R_a^2 = \epsilon_e R_e^2\,.$$

The redshift according to (5) is then

$$1 + z = \frac{R_e^2\,\epsilon_e\,\frac{c}{R_e}}{R_a^2\,\epsilon_a\,\frac{c}{R_a}} = \frac{R_a}{R_e}\,.$$

Thus, wavelengths obey the same scaling law as distances within spatial slices of constant cosmological time. Phenomenologically, the light wave gets stretched alongside the metric expansion of space.

[13] this follows from the normalization condition

[14] derivation of the Christoffel symbols for this simple metric is not particularly hard or enlightening and will not be shown

4.3 Schwarzschild Spacetime and Gravitational Redshift

The frequency shift within Schwarzschild spacetime is known as gravitational redshift, though in case of ingoing photons, the shift will of course occur towards shorter wavelengths[15]. Phenomenologically, the photon will lose or gain energy by climbing out or falling into the gravitational potential well.

Starting point for the discussion is the Schwarzschild metric in reduced circumference polar coordinate is given by[16]

$$\mathrm{d}\, s^2 = -\left(1 - \frac{r_s}{r}\right) c^2\, \mathrm{d}\, t^2 + \left(1 - \frac{r_s}{r}\right)^{-1} \mathrm{d}\, r^2 + r^2\, \mathrm{d}\, \Omega^2$$

with $\mathrm{d}\,\Omega$ as in last section and $r_s = 2Gm/c^2$ denoting the Schwarzschild radius, a convenient reimagining of the black hole mass m as a length scale.

The situation under investigation is a photon travelling radially outwards from a source sitting at fixed Schwarzschild coordinates with radius r_e towards an observer also sitting at fixed coordinates and at a greater radius r_a.

In terms of parallel transport of momentum, the discussion would proceed almost identically as the last case of cosmological redshift[17]. However, given that the Schwarzschild spacetime is stationary - as can be seen explicitly by the lack of time dependence of the metric - it is far more convenient to look at wave front timings instead of solving parallel transport equations.

So let the source emit a wavefront. Let the coordinate time taken to reach the observer be ΔT_1. After a time Δt_e, a second wave front gets emitted, travelling towards the observer in time ΔT_2. The coordinate time that has passed since the arrival of the previous wave front is given by

$$\Delta t_a = \Delta t_e + \Delta T_2 - \Delta T_1\,.$$

While the travelling time of the wave is unknown, what is known is that $\Delta T_1 = \Delta T_2$ as the background metric has not changed, and thus one also has $\Delta t_a = \Delta t_e$.

All that remains to do is to translate coordinate time into proper times of source and observer. The time dilation can be read from the metric via $\mathrm{d}\, s^2 = -c^2\, \mathrm{d}\, \tau^2$. At fixed spatial coordinates, this reduces to

$$\mathrm{d}\, \tau^2 = \left(1 - \frac{r_s}{r}\right) \mathrm{d}\, t^2$$

[15] arguably, the name is not ideal for other reasons as well: Take cosmological redshift as an example, which is also a consequence of spacetime curvature, i.e. the presence of gravity

[16] see eg [3, ch. 14.5] or any other introductory book on General Relativity

[17] the reduced metric of the problem can be made to look almost identical by use of the 'tortoise' coordinate $r^\star$ (see eg. [12, p. 663]), except that the conformal factor would have a spatial dependence $R = R(\chi)$ instead

and thus

$$\Delta\tau = \sqrt{1 - \frac{r_s}{r}}\Delta t$$

The redshift will be given by

$$1 + z = \frac{\Delta\tau_a}{\Delta\tau_e} = \sqrt{\frac{1 - r_s/r_a}{1 - r_s/r_e}}$$

In this case, the frequency shift can be attributed wholly to gravitational time dilation, a result that also follows immediately from section 3.3.

5 Kerr-de Sitter Spacetime

The following section introduces the metric of Kerr-de Sitter spacetime, describing a rotating black hole embedded in a universe that isn't asymptotically flat, but, like our own, features a nonzero cosmological constant. It is part of the Plebański-Demiański family of solutions to the Einstein equations [14][6], which can be used to model a variety of physical situation (cosmological constant, massive black holes carrying electric and magnetic charge, rotating black holes, accelerating black holes, NUT charge). While not as general, the Kerr-de Sitter solution is no mere toy model and exhibits several interesting features. This particular expression for the metric has been generalized by Gibbons, Lü, Page and Pope in [5] to arbitrary dimensions.

The contents of this section are largely technical. From here on out, factors of c will be dropped for notational convenience.

5.1 Spheroidal Coordinates

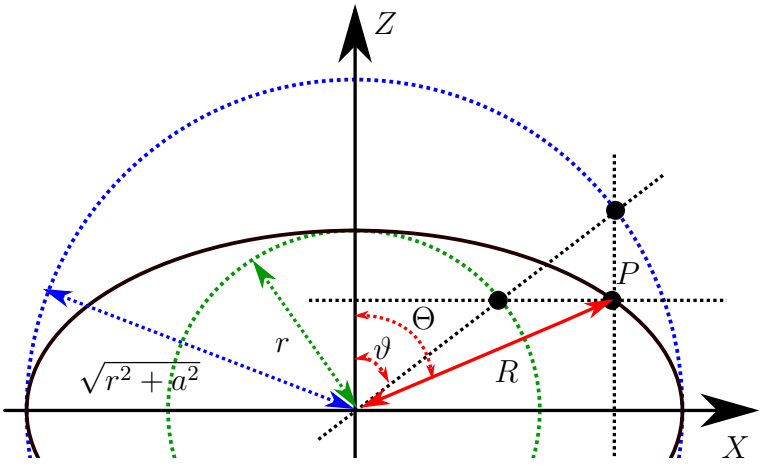

Figure 2: Parametrization of an ellipse through a point P and relation to spherical coordinates

Rotating black holes break the spatial symmetry of spacetime from spherically to axially symmetric. This formulations of the metric makes use of a spheroidal coordinate system that also has that such symmetry.

Let Cartesian coordinates be denoted by X, Y, Z and spherical coordinates by R, Θ, φ. Due to axial symmetry, we restrict the discussion to the XZ-plane. For a fixed linear eccentricity a, there is a unique ellipse centered at the origin through any point P. Let r denote the semi-minor axis of that ellipse. Its semi-major axis will take

the value $\sqrt{r^2+a^2}$, and the whole ellipse can be parametrized by an angle ϑ via[18]

$$\begin{aligned} X &= \sqrt{r^2+a^2}\sin\vartheta \\ Z &= r\cos\vartheta\,, \end{aligned}$$

which is shown in figure 2.

For each value of a, a spheroidal coordinate system is given by the set r, ϑ, φ. The transformation to spherical coordinates is given by

$$\begin{aligned} R\sin\Theta &= \sqrt{r^2+a^2}\sin\vartheta \\ R\cos\Theta &= r\cos\vartheta \end{aligned}$$

from which we can also derive

$$\begin{aligned} R^2 &= (r^2+a^2)\sin^2\vartheta + r^2\cos^2 \\ &= r^2 + a^2\sin^2\vartheta\,. \end{aligned}$$

In our new coordinates, the Euclidean metric takes the form

$$\mathrm{d}\,s^2 = \frac{r^2+a^2\cos^2\vartheta}{r^2+a^2}\,\mathrm{d}\,r^2 + (r^2+a^2\cos^2\vartheta)\,\mathrm{d}\,\vartheta^2 + (r^2+a^2)\sin^2\vartheta\,\mathrm{d}\,\varphi^2$$

or, introducing a new coordinate $\chi = \cos\vartheta$ to avoid trigonometric expressions

$$\mathrm{d}\,s^2 = \frac{r^2+a^2\chi^2}{r^2+a^2}\,\mathrm{d}\,r^2 + \frac{r^2+a^2\chi^2}{1-\chi^2}\,\mathrm{d}\,\chi^2 + (r^2+a^2)(1-\chi^2)\,\mathrm{d}\,\varphi^2\,.$$

The equivalence of this metric to the expression in spherical coordinates is shown explicitly in appendix A.1.

5.2 De Sitter Spacetime in Spheroidal Coordinates

The metric of de Sitter spacetime describing a homogeneous isotropic universe without matter, but non-vanishing cosmological constant. It can be expressed as

$$\mathrm{d}\,s^2 = -(1-\lambda R^2)\,\mathrm{d}\,t^2 + \left(1-\lambda R^2\right)^{-1}\mathrm{d}\,R^2 + R^2\,\mathrm{d}\,\Theta^2 + R^2\sin^2\Theta\,\mathrm{d}\,\varphi^2$$

where $\lambda = \alpha^{-2}$ in terms of the de Sitter radius α and $\lambda = \Lambda/3$ in terms of the cosmological constant Λ.

The transformation to spheroidal coordinates will be adjusted from the previous section to account for the presence of λ. It is given by

$$\begin{aligned} R\sin\Theta &= \sqrt{\frac{(r^2+a^2)\,(1-\chi^2)}{1+\lambda a^2}} \\ R\cos\Theta &= r\chi \end{aligned}$$

[18] this construction goes back to the mathematician Philippe de La Hire

and thus

$$R^2 = \frac{(r^2+a^2)\,(1-\chi^2)}{1+\lambda a^2} + r^2\chi^2\,.$$

Expressed in these coordinates, the metric for de Sitter spacetime reads

$$\begin{aligned}\mathrm{d}\,s^2 = &-\frac{(1-\lambda r^2)\,(1+\lambda a^2\chi^2)}{1+\lambda a^2}\,\mathrm{d}\,t^2 + \frac{r^2+a^2\chi^2}{(1-\lambda r^2)\,(r^2+a^2)}\,\mathrm{d}\,r^2 \\ &+ \frac{r^2+a^2\chi^2}{(1+\lambda a^2\chi^2)\,(1-\chi^2)}\,\mathrm{d}\,\chi^2 + \frac{(r^2+a^2)\,(1-\chi^2)}{1+\lambda a^2}\,\mathrm{d}\,\varphi^2\,.\end{aligned} \tag{9}$$

Note that physically, nothing has happened yet: The metric still describes de Sitter spacetime, merely in a more unwieldy form. This will change in the subsection following the next one.

5.3 Construction of Derived Metrics in Kerr-Schild Form

The construction mechanism will only be sketched instead of described in detail.

A metric $\mathrm{d}\,s^2$ is said to be in Kerr-Schild form when it has been written as

$$\mathrm{d}\,s^2 = \mathrm{d}\,s_0^2 + hk_\mu k_\nu\,\mathrm{d}\,x^\mu\,\mathrm{d}\,x^\nu$$

where $\mathrm{d}\,s_0^2$ is some base metric,[19] h some function and k_μ a covector field that is null regarding $\mathrm{d}\,s_0^2$.

This ansatz has been first studied by Trautman during the investigation of gravitational waves [20] with important results by Kerr and Schild [9][10] and further studies by Gürses and Gürsey [7][2] and others.

Let $\mathrm{d}\,s_0^2 = \bar{g}_{\mu\nu}\,\mathrm{d}\,x^\mu\,\mathrm{d}\,x^\nu$ and $k^\mu := (k^\mu)_{s_0} = \bar{g}^{\mu\nu}k_\nu$. Then $g^{\mu\nu}$ is given by

$$g^{\mu\nu} = \bar{g}^{\mu\nu} - hk^\mu k^\nu$$

because

$$(\bar{g}^{\mu\lambda} - hk^\mu k^\lambda)(\bar{g}_{\lambda\nu} + hk_\lambda k_\nu) = \bar{g}^{\mu\lambda}\bar{g}_{\lambda\nu} = \delta^\mu_\nu\,.$$

This also implies

$$k^\mu = g^{\mu\nu}k_\nu = (k^\mu)_s\ ,$$

meaning k^μ is a null vector field respective to either metric.

This has important consequences:

For one, k^μ is geodesic with respect to $\mathrm{d}\,s^2$ if and only if it is geodesic with respect to $\mathrm{d}\,s_0^2$. Also, it is necessarily geodesic if $\mathrm{d}\,s^2$ solves the vacuum Einstein equations [18, ch. 32].[20]

[19] often, but not necessarily the Minkowski metric

[20] in the presence of matter, we additionally must have $T_{\mu\nu}k^\mu k^\nu = 0$

On the flip side, if k^μ is a null-geodesic congruence and $\mathrm{d}\, s_0^2$ solves the Einstein equations, $h_{\mu\nu} := h k_\mu k_\nu$ only needs to solve the Einstein equations linearized[21] around $\mathrm{d}\, s_0^2$ for $\mathrm{d}\, s^2$ to solve the full Einstein equations [2].

The final step of this proof has been provided as appendix A.2.

5.4 Schwarzschild Spacetime in Kerr-Schild Form

To illustrate the mechanism, Schwarzschild spacetime in Kerr-Schild form will be constructed, starting from the Minkowski metric in spherical coordinates:

$$\mathrm{d}\, s_0^2 = -\,\mathrm{d}\, t^2 + \mathrm{d}\, r^2 + r^2\,\mathrm{d}\,\vartheta + \mathrm{d}\,\Omega^2$$

Choosing radial null geodesics oriented towards the past as congruence, the vector field takes the form

$$k^\mu \partial_\mu = -\partial_t + \partial_r$$

with corresponding covectorfield

$$k_\mu\,\mathrm{d}\, x^\mu = \mathrm{d}\, t + \mathrm{d}\, r.$$

Let r_s be a characteristic length and

$$h = \frac{r_s}{r}$$

and thus

$$h_{\mu\nu}\,\mathrm{d}\, x^\mu\,\mathrm{d}\, x^\nu = \frac{r_s}{r}\left(\mathrm{d}\, t^2 + \mathrm{d}\, r^2 + 2\,\mathrm{d}\, t\,\mathrm{d}\, r\right) .$$

The new metric $\mathrm{d}\, s^2 = \mathrm{d}\, s_0^2 + h_{\mu\nu}\,\mathrm{d}\, x^\mu\,\mathrm{d}\, x^\nu$ will then be given by

$$\mathrm{d}\, s^2 = -\left(1 - \frac{r_s}{r}\right)\mathrm{d}\, t^2 + \left(1 + \frac{r_s}{r}\right)\mathrm{d}\, r^2 + 2\frac{r_s}{r}\,\mathrm{d}\, t\,\mathrm{d}\, r + \mathrm{d}\,\Omega^2$$

To show that this is a solution to the Einstein equation, one only needs to check that $h_{\mu\nu}$ fulfills the linearized equation given in appendix A.2. This will not be presented. Instead, the metric can be brought into standard form by the coordinate transformation

$$t_{\text{Schwarzschild}} = t - r_s \ln\left|\frac{r}{r_s} - 1\right|$$

That calculation can be found in appendix A.3.

[21] to prove this, h can be formally replaced by ϵh and all derived quantities expanded in powers of ϵ

5.5 Kerr-de Sitter Spacetime in Kerr-Schild Form

The derivation of the Kerr-de Sitter metric in Kerr-Schild form proceeds analogously to the last section, but starts with the de Sitter metric in spheroidal coordinates (9), using a null geodesic congruence

$$k^\mu \partial_\mu = -\frac{1}{1-\lambda r^2}\partial_t + \partial_r - \frac{a}{r^2+a^2}\partial_\varphi$$

and h given by

$$h = \frac{r_s r}{r^2 + a^2\chi^2}\,.$$

The covector k_μ becomes

$$k_\mu \,\mathrm{d}\, x^\mu = \frac{1+\lambda a^2\chi^2}{1-\lambda a^2}\,\mathrm{d}\, t + \frac{r^2+a^2\chi^2}{(1-\lambda r^2)\,(r^2+a^2)}\,\mathrm{d}\, r - \frac{a(1-\chi^2)}{1+\lambda a^2}\,\mathrm{d}\,\varphi$$

Putting this all together, the Kerr-de Sitter metric in expanded Kerr-Schild form is

$$\begin{aligned}
\mathrm{d}\, s^2 = &-\frac{1+\lambda a^2\chi^2}{1+\lambda a^2}\left(1-\lambda r^2 - \frac{r r_s(1+\lambda a^2\chi^2)}{(1+\lambda a^2)\,(r^2+a^2\chi^2)}\right)\mathrm{d}\, t^2 \\
&+ \frac{r^2+a^2\chi^2}{(1-\lambda r^2)\,(r^2+a^2)}\left(1+\frac{r r_s}{(1-\lambda r^2)\,(r^2+a^2)}\right)\mathrm{d}\, r^2 \\
&+ \frac{r^2+a^2\chi^2}{(1+\lambda a^2\chi^2)\,(1-\chi^2)}\,\mathrm{d}\,\chi^2 \\
&+ \frac{1-\chi^2}{1+\lambda a^2}\left(r^2+a^2+\frac{r r_s a^2(1-\chi^2)}{(1+\lambda a^2)\,(r^2+a^2\chi^2)}\right)\mathrm{d}\,\varphi^2 \\
&+ 2 r r_s \frac{1+\lambda a^2\chi^2}{(1+\lambda a^2)\,(1-\lambda r^2)\,(r^2+a^2)}\,\mathrm{d}\, t\,\mathrm{d}\, r \\
&- 2 r r_s \frac{a(1+\lambda a^2\chi^2)\,(1-\chi^2)}{(1+\lambda a^2)^2\,(r^2+a^2\chi^2)}\,\mathrm{d}\, t\,\mathrm{d}\,\varphi \\
&- 2 r r_s \frac{a(1-\chi^2)}{(1+\lambda a^2)\,(1-\lambda r^2)\,(r^2+a^2)}\,\mathrm{d}\, r\,\mathrm{d}\,\varphi
\end{aligned}$$

This is not a mere reformulation of the flat vacuum solution, but a wholly distinct curved system. The new parameter r_s, the formerly arbitrary and only cosmetic parameter a, and the parameter λ inherited from de Sitter spacetime now represent the physical quantities black hole mass, angular momentum and cosmological constant.

For $\lambda = 0$, we recover a variant of the Kerr metric, which describes rotating black holes in asymptotically flat spacetime, given by

$$\begin{aligned}
\mathrm{d}\, s^2 = &-\left(1-\frac{r r_s}{r^2+a^2\chi^2}\right)\mathrm{d}\, t^2 + \frac{r^2+a^2\chi^2}{r^2+a^2}\left(1+\frac{r r_s}{r^2+a^2}\right)\mathrm{d}\, r^2 \\
&+ \frac{r^2+a^2\chi^2}{1-\chi^2}\,\mathrm{d}\,\chi^2 + (1-\chi^2)\left(r^2+a^2+\frac{r r_s a^2(1-\chi^2)}{r^2+a^2\chi^2}\right)\mathrm{d}\,\varphi^2 \\
&+ 2 r r_s \frac{1}{r^2+a^2}\,\mathrm{d}\, t\,\mathrm{d}\, r - 2 r r_s \frac{a(1-\chi^2)}{r^2+a^2\chi^2}\,\mathrm{d}\, t\,\mathrm{d}\,\varphi - 2 r r_s \frac{a(1-\chi^2)}{r^2+a^2}\,\mathrm{d}\, r\,\mathrm{d}\,\varphi
\end{aligned}$$

Note that the tt-component changes its sign at

$$r_\pm = \frac{r_s}{2} \pm \sqrt{\frac{r_s^2}{4} - a^2\chi^2}.$$

which defines the so-called ergospheres of a rotating black hole. In contrast, the event horizons, of which there are now two, are not manifestly present.

The linearization of the Einstein equations will again not be presented. Instead, it has been verified that the metric above does indeed fulfill the Einstein equations via the computer algebras system *SageMath* [19][17].[22] The Christoffel symbols have been obtained that way as well. Some exemplary terms have been rendered in appendix A.4.

[22] the code is a mere `R = g.ricci(); S = g.ricci_scalar(); R - 0.5*S*g + 3*lm*g == 0`, with `g` the metric above and `lm` a parameter

6 Simulation Methodology

This section briefly describes the algorithms used to advance photon state and calculate redshift, but merely in the abstract. Details of the programmatic implementation in C are not provided.

From now on, photon velocity will be denoted by v^μ.

6.1 Integration Method

The following leapfrog integrator in kick-drift-kick form was used to iterate the equations of motion (2) from timestep $i \to i+1$:

$$\begin{aligned}
\left[v^\mu\right]_{i+1/2} &= \left[v^\mu\right]_i - \left[\Gamma^\mu_{\alpha\beta} v^\alpha v^\beta\right]_i \frac{\Delta t}{2} \\
\left[x^\mu\right]_{i+1} &= \left[x^\mu\right]_i + \left[v^\mu\right]_{i+1/2} \Delta t \\
\left[v^\mu\right]_{i+1} &= \left[v^\mu\right]_{i+1/2} - \left[\Gamma^\mu_{\alpha\beta}\right]_{i+1} \left[v^\alpha v^\beta\right]_{i+1/2} \frac{\Delta t}{2}
\end{aligned}$$

It is a second order symplectic integrator which has seen successful application in many fields of physics such as molecular dynamics [1]. The particular implementation developed for this thesis dynamically adapts the timestep size when spatial resolution becomes too coarse. It would be preferable to perform this in a systematic manner to avoid negative impacts on numeric stability [15], but this is beyond the scope of this thesis.

6.2 Computation of the Frequency Shift

As the geodesic equation is used to iterate photon position and velocity, there is no need to explicitly parallel transport the momentum vector. Instead, equation (6) is used. All observations will be made in the Kerr-de Sitter coordinate frame, i.e. observers sitting still at fixed coordinates (r, χ, φ). The expressions for such velocities have already been given in section 3.3.

The redshift at timestep i is computed from current values and initial value at step 0 via

$$\left[1+z\right]_i = \frac{\left[\dfrac{g_{0\mu} v^\mu}{\sqrt{-g_{00}}}\right]_0}{\left[\dfrac{g_{0\nu} v^\nu}{\sqrt{-g_{00}}}\right]_i} .$$

Conservation of canonical energy has not been leveraged. This means arbitrary time-dependent metrics can be supported.

Note that choice of using the coordinate frame for observation has severe limitations, which will be pointed out when relevant.

6.3 Graphical Representation

The spatial slices of constant time are in general non-Euclidean, so any coordinate choice will give a distorted picture by necessity. It was decided to undo the coordinate change to spheroidal coordinates described in section 5.2. This recovers the inner structure of the Kerr black hole as conventionally rendered in Cartesian Kerr-Schild coordinates [21]. If the spheroidal coordinates had naively been rendered, the ring singularity would have collapsed to a point.

In case of Schwarzschild black holes, the event horizon will be rendered graphically, in case of Kerr black holes, the outer event horizon and ergosphere.

7 Simulation Results

The results presented in this section either demonstrate a particular physical effect of interest or showcase an issue with the numeric approach taken. In order, closed photon orbits in Schwarzschild and Kerr Spacetime, energy and angular momentum drift in Kerr spacetime, gravitational redshift in Schwarzschild and Schwarzschild-de Sitter spacetime, and finally, crossing the event horizon into the interior of a Kerr black hole will be discussed briefly.

All black holes will have a mass parameter $r_s = 1$, which serves as fundamental length scale in all examples.

7.1 Photon Orbits in Schwarzschild and Kerr Spacetime

In both Schwarzschild and Kerr Spacetime, there exist closed photon orbits. For Kerr spacetime, the pro- and retrograde orbits are distinct and given by [13]

$$r_{\mathrm{po}} = r_s \left(1 + \cos\left(\frac{2}{3} \arccos \frac{\mp 2a}{r_s}\right)\right) .$$

This is consistent with the result for Schwarzschild spacetime

$$r_{\mathrm{po}} = 1.5\, r_s.$$

Figure 3 shows the result for parameters $r_s = 1$ and, in case of the Kerr black hole, $a = 0.499$.

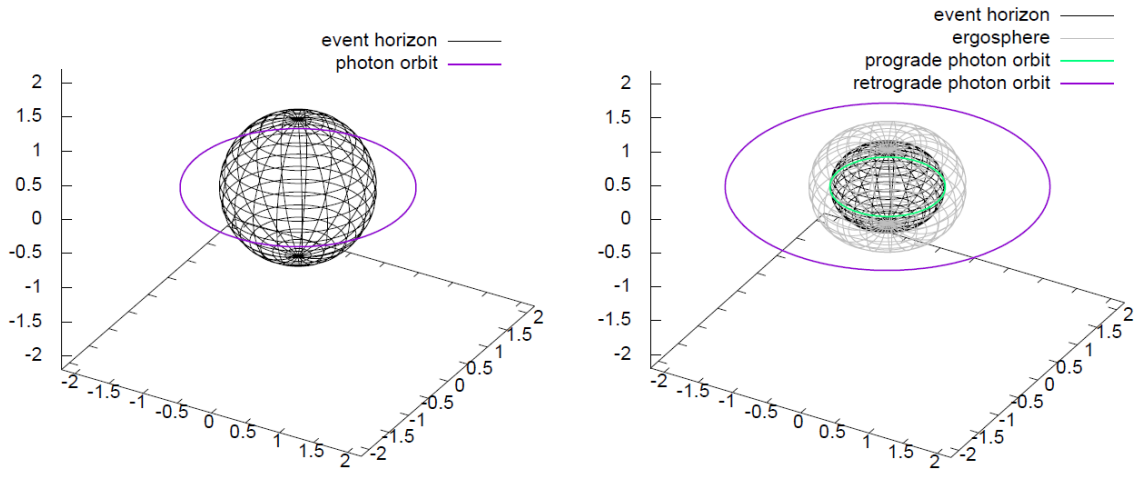

Figure 3: Photon orbits in Schwarzschild (left) and Kerr spacetime (right)

The Schwarzschild and retrograde Kerr orbits showed no numeric drift at all. The prograde orbit did drift. Figure 4 shows a sampling of photon position in the xy-plane, with colour indicating sequence number. After an initial meta-stable period,

the photon jumped into a new orbit. To understand what is going on, the squarenorm of photon velocity - which should be a constant of motion - has been plotted in figure 5.

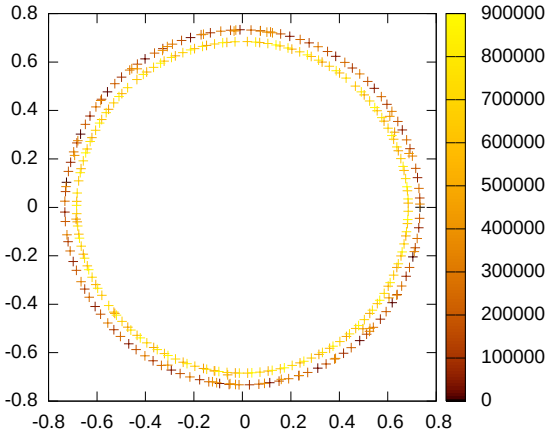

Figure 4: Sampling of positions of photon in retrograde Kerr orbit

The squarenorm shows the same characteristic evolution as the photon position. A metastable phase **A** with small drift experiences a perturbation, resulting in a phase **B** of rapid change until a new metastable phase **C** with small drift has been entered. Looking at the sign, a timelike velocity indicates that the photon started with a small mass. After the switch in metastable states, the velocity is now spacelike, and the photon now technically a tachyon.

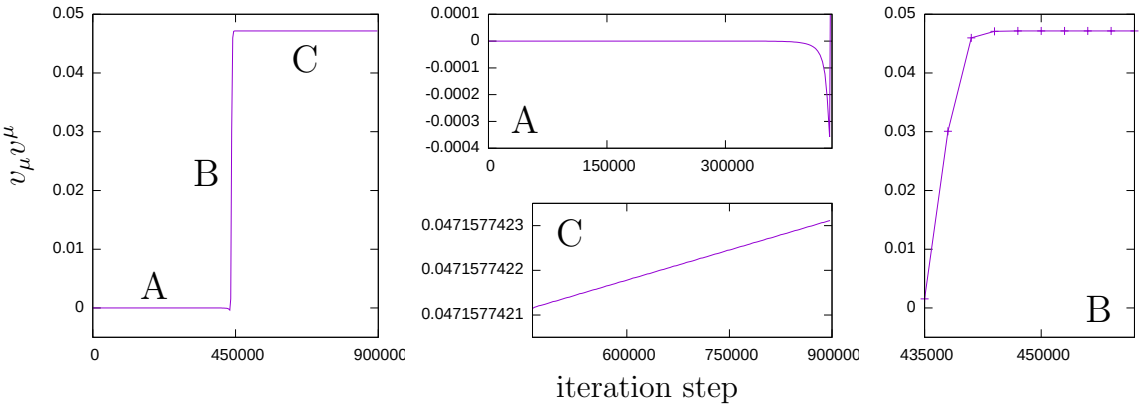

Figure 5: Evolution of the squarenorm of photon velocity

7.2 Energy and Angular Momentum Drift in Kerr Spacetime

According to section 3.3, canonical energy and axial angular momentum

$$E = g_{0\mu}v^{\mu} \qquad L = g_{4\mu}v^{\mu}$$

are conserved quantities in Kerr spacetime. Figure 6 shows a visually appealing trajectory around a black hole with rotation parameter $a = 0.4$. Figure 7 shows the drift in the supposedly conserved canonical energy and angular momentum around the symmetry axis.

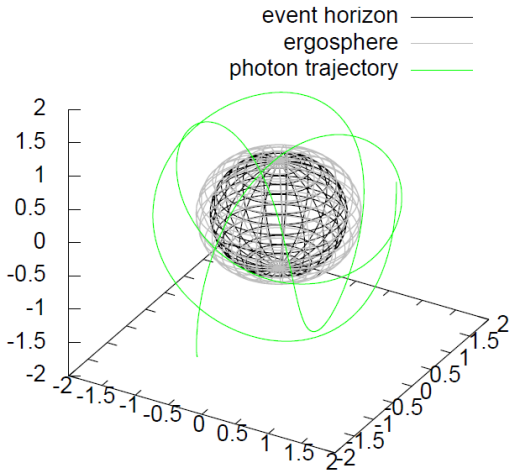

Figure 6: One of many interesting photon trajectory around a Kerr black hole

A certain amount of numeric drift is hard to avoid, though the result could likely be improved by choosing an integrator that has been specialized for velocity-dependent forces. It might also be possible to improve the situation by choosing coordinates derived from cylindrical instead of spherical coordinates, explicitly respecting the symmetry of the system.

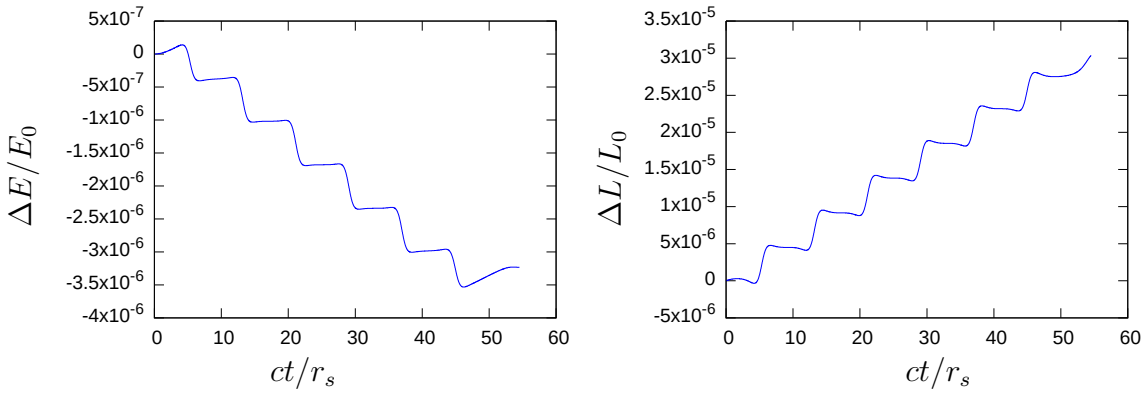

Figure 7: Relative energy and angular momentum drift

7.3 Gravitational Redshift in Schwarzschild Spacetime

The analytical expression for gravitational redshift has been derived in section 4.3. Figure 8 shows the numeric result for an outgoing photon emitted at a radius of $1.2r_s$ and absorbed at a radius of $6.2r_s$ as well as an ingoing twin.

The deviation from the analytical result is not the same for the ingoing and outgoing case: The ingoing value rapidly swings into the correct values, whereas the outgoing photon shows the greater deviation and continues to show a systematic error. A possible explanation is the lack of step size adjustment: The errors are expected to be greatest closest to the event horizon, where gradients are maximal and an initially accumulated offset cannot be compensated later on.

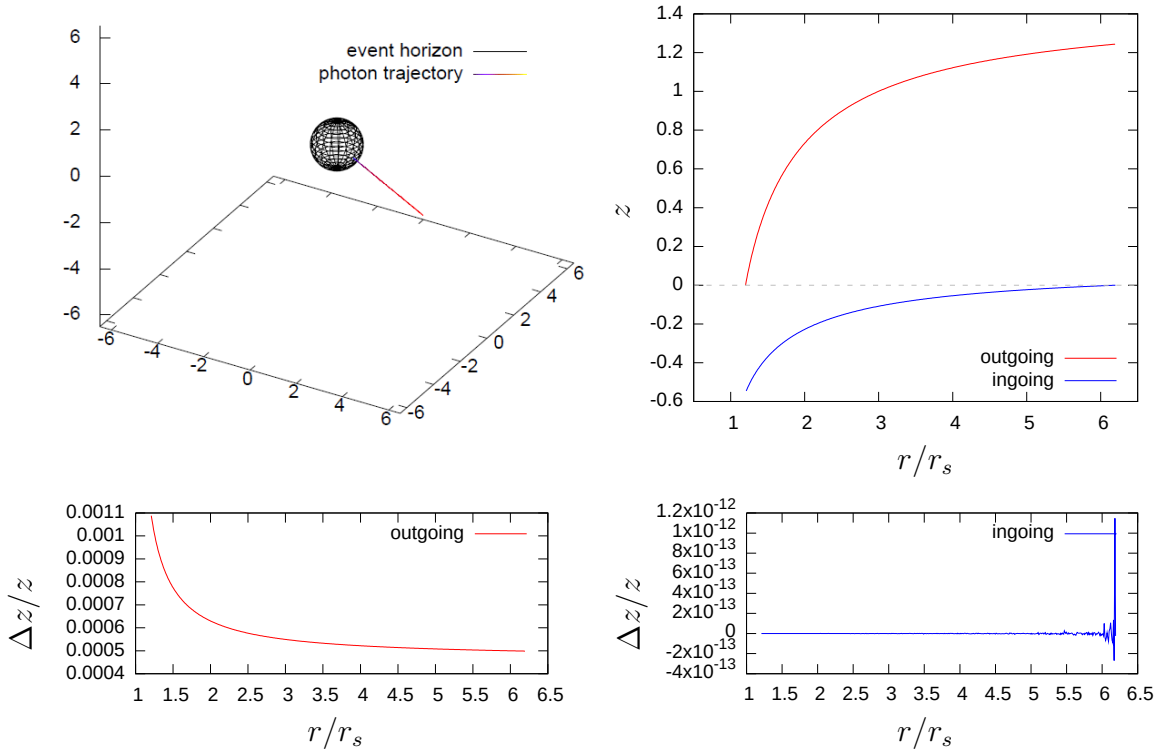

Figure 8: Photon trajectory, gravitational redshift and relative deviations from analytical expression

When switching on a positive cosmological constant, in the parameter range chosen, the photon will be sandwiched between black hole and cosmological horizon, located at [13]

$$r_{\pm} = \frac{2}{\sqrt{\Lambda}} \cos\left[\frac{\pi}{3} \pm \frac{1}{3} \arccos\left(\frac{3r_s}{2}\sqrt{\Lambda}\right)\right]$$

Figure 9 shows what happens to redshift in this situation. There appears to be a radius where redshift becomes independent of the parameter $\Lambda = 3\lambda$.

However, when trying to relate results to direct experience, the limitation of fixing just one observer strikes: Of interest are primarily observers that are comoving with

the Hubble flow in an expanding universe instead of some the chosen observer sitting in a seemingly static universe. The question of how the two observes are related has not been considered in this work, though.

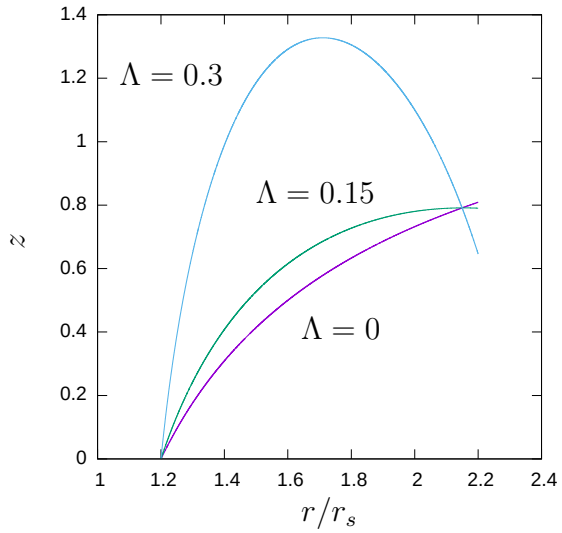

Figure 9: Redshift in Schwarzschild-de Sitter spacetime with varying cosmological constant

7.4 Probing the Interior of Kerr Black Holes

Rotating black holes have rich interior structure, and the coordinates used here remain useable while crossing the outer horizons until the singularity is hit. However, graphical representation will be misleading as various coordinates exchange their quality, time becoming spacelike and spacelike coordinates becoming timelike. This is also a problem when calculating the frequency shift, as naively, photon energy would become imaginary. To obtain sensible results, a different observer would have to be chosen.

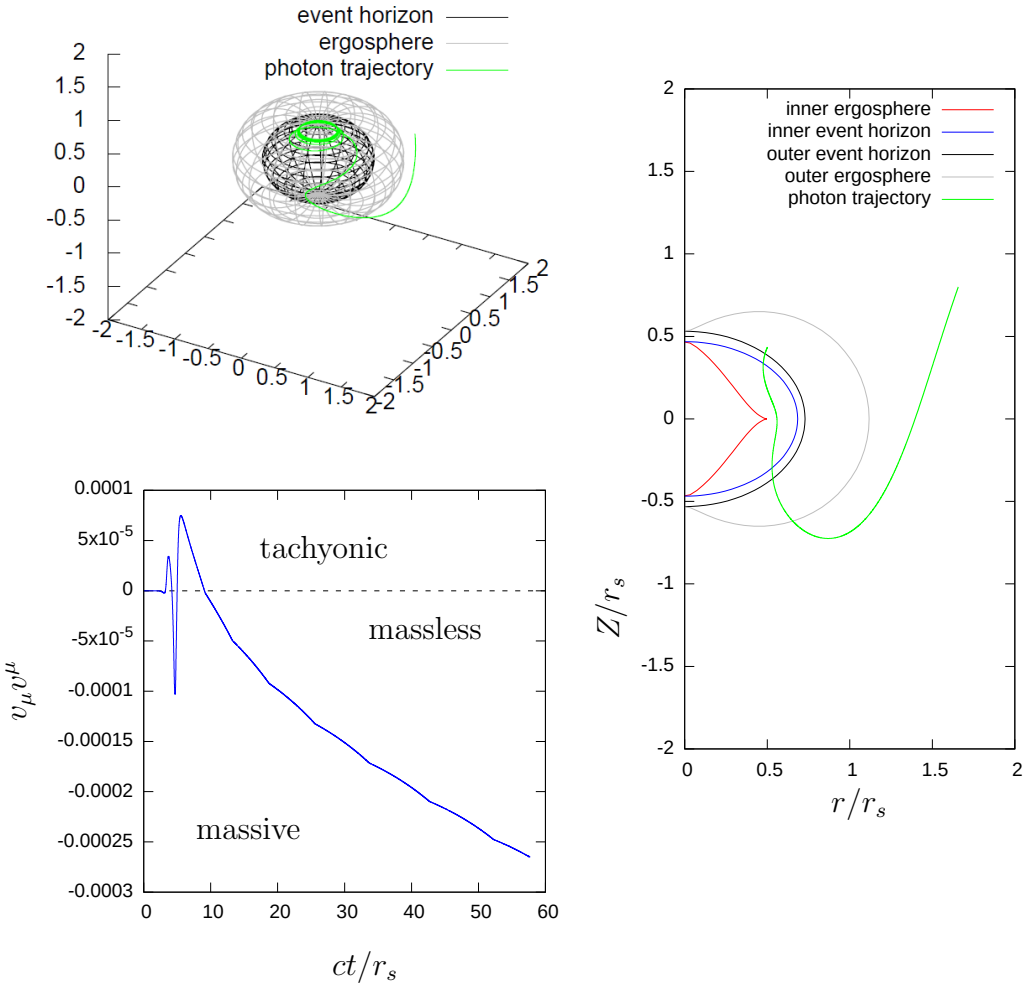

Figure 10: Photon trajectory entering a Kerr black hole, with radial plot on the right and square of photon velocity bottom left

Figure 10 shows the trajectory of a photon that enters a rotating black hole with $a = 0.499$. The singularity located at the cusp of the inner ergosphere has been avoided. However, the photon then proceeds to re-cross both inner and outer event horizon before happily orbiting within the outer ergosphere. The bottom left graph shows the photon's velocity squared, giving a hint why this is possible: At various

points in time, the photon became spacelike, and this temporary tachyonic nature allows it to enter classically forbidden regions.

An option might be to use a family of massive particles with decreasing mass to numerically probe the structure of spacetime, instead of using photons that will generally not behave entirely correctly, as they will keep switching between massive and tachyonic behaviour instead of being massless.

8 Conclusion

In this work, relativistic frequency shifts have been explored both conceptionally and via simple hands-on calculations. It has been argued that these shifts can be regarded as a kinematic consequence of curved spacetime, irrespective of any phenomenological explanation. Parallel transport of photon momentum is sufficient to explain all different cases, as is the naive approach of tracking wave fronts, though the latter has several shortcomings and is unsuitable for computational analysis.

Kerr-de Sitter spacetime was chosen as a proper subject for numerical investigation of relativistic frequency shifts. Therefore, an expression for the metric tensor and its Christoffel symbols had to be obtained. The derivation of the metric via a Kerr-Schild ansatz was sketched.

Some generic results regarding numeric simulation were presented, and a few simple cases of redshift have been modelled. The existence of an apparent fixed point of redshift in Schwarzschild-de Sitter spacetime irrespective of the value of the cosmological constant was genuine news to the author, but may very well be well-established in the literature.

The most interesting goal of exploring Kerr-de Sitter phenomenology in detail has to be deferred to potential subsequent work: The initial decision to restrict investigation to timelike geodesics and the pragmatic decision to initially only consider the frame induced by the chosen coordinates limited the scope of the investigation.

If future work were to be performed, the addition of other classes of observers should be considered. The use of timelike geodesics to obtain the behavior of null-geodesics as a limit might be wothwhile to persue, in hope that it will suffer less from the horizon-jumping tendencies of photons that easily slip into tachyonic behaviour.

A Appendix

A.1 Equivalence of Spherical and Spheroidal Metrics

The Euclidian metric in spherical coordinates can be rewritten into

$$\mathrm{d}\,s^2 = \mathrm{d}\,R^2 + \frac{R^2}{1-\eta^2}\,\mathrm{d}\,\eta^2 + R^2(1-\eta^2)\,\mathrm{d}\,\varphi^2$$

by introducing $\eta = \cos\Theta$. The non-trivial part one needs to show is that

$$\mathrm{d}\,R^2 + \frac{R^2}{1-\eta^2}\,\mathrm{d}\,\eta^2 = \frac{r^2+a^2\chi^2}{r^2+a^2}\,\mathrm{d}\,r^2 + \frac{r^2+a^2\chi^2}{1-\chi^2}\,\mathrm{d}\,\chi^2 \tag{10}$$

Recalling the definitions of section 5.1, we have

$$\begin{aligned} R\eta &= r\chi \\ R^2 &= r^2 + a^2(1-\chi^2) \end{aligned}$$

from which one can derive

$$\begin{aligned} \mathrm{d}\,\eta &= \frac{\chi}{R}\,\mathrm{d}\,r + \frac{r}{R}\,\mathrm{d}\,\chi - \frac{r\chi}{R^2}\,\mathrm{d}\,R \\ \mathrm{d}\,R &= \frac{r}{R}\,\mathrm{d}\,r - \frac{a^2\chi}{R}\,\mathrm{d}\,\chi \\ \frac{1}{1-\eta^2} &= \frac{R^2}{(r^2+a^2)(1-\chi^2)}\,. \end{aligned}$$

Plugging this into (10) yields

$$\begin{aligned} (\mathrm{LHS}) &= (\ldots \text{the cross terms cancel} \ldots) \\ &= \left(\frac{r^2}{R^2} + \frac{a^4\chi^2(1-\chi^2)}{R^2(r^2+a^2)}\right)\mathrm{d}\,r^2 + \left(\frac{a^4\chi^2}{R^2} + \frac{r^2(r^2+a^2)}{R^2(1-\chi^2)}\right)\mathrm{d}\,\chi^2 \\ &= (\ldots \text{add fractions, expand and re-factorize} \ldots) \\ &= \frac{R^2(r^2+a^2\chi^2)}{R^2(r^2+a^2)}\,\mathrm{d}\,r^2 + \frac{R^2(r^2+a^2\chi^2)}{R^2(1-\chi^2)}\,\mathrm{d}\,\chi^2 \\ &= (\mathrm{RHS}) \end{aligned}$$

using elementary algebra.

A.2 Linearized Einstein Equations

According to [2], linearization yields the Ricci tensor

$$R^{\mu}_{\nu} = \bar{R}^{\mu}_{\nu} - h^{\mu}_{\alpha}R^{\alpha}_{\nu} + \frac{1}{2}\left(\bar{\nabla}_{\alpha}\bar{\nabla}_{\nu}h^{\mu\alpha} + \bar{\nabla}^{\alpha}\bar{\nabla}^{\mu}h_{\nu\alpha} - \bar{\nabla}^{\alpha}\bar{\nabla}_{\alpha}h^{\mu}_{\nu}\right) .$$

Tracing over the vacuum Einstein equations for $\bar{g}_{\mu\nu}$ and raising one of the indices, we have

$$\bar{R} = 4\Lambda \qquad\qquad \bar{R}^{\mu}_{\nu} = (\frac{1}{2}\bar{R} - \Lambda)\delta^{\mu}_{\nu} = \Lambda\delta^{\mu}_{\nu} .$$

Additionally using $h^{\mu}_{\mu} = 0$, we also have

$$R = 4\Lambda + \bar{\nabla}_{\alpha}\bar{\nabla}_{\beta}h^{\alpha\beta}$$

and arrive at the linearized Einstein equation

$$\begin{aligned} 0 &= \Lambda\delta^{\mu}_{\nu} - \Lambda h^{\mu}_{\nu} + \frac{1}{2}\left(\bar{\nabla}_{\alpha}\bar{\nabla}_{\nu}h^{\mu\alpha} + \bar{\nabla}^{\alpha}\bar{\nabla}^{\mu}h_{\nu\alpha} - \bar{\nabla}^{\alpha}\bar{\nabla}_{\alpha}h^{\mu}_{\nu}\right) - \frac{1}{2}(4\Lambda + \bar{\nabla}_{\alpha}\bar{\nabla}_{\beta}h^{\alpha\beta})\delta^{\mu}_{\nu} + \Lambda\delta^{\mu}_{\nu} \\ &= \frac{1}{2}\left(\bar{\nabla}_{\alpha}\bar{\nabla}_{\nu}h^{\mu\alpha} + \bar{\nabla}^{\alpha}\bar{\nabla}^{\mu}h_{\nu\alpha} - \bar{\nabla}^{\alpha}\bar{\nabla}_{\alpha}h^{\mu_{\nu}} - \delta^{\mu}_{\nu}\bar{\nabla}_{\alpha}\bar{\nabla}_{\beta}h^{\alpha\beta}\right) - \Lambda h^{\mu}_{\nu} \end{aligned}$$

A.3 Recovery of Schwarzschild Metric from Kerr-Schild Form

It is sufficient to show that

$$\begin{aligned} &-\left(1-\frac{r_s}{r}\right)\mathrm{d}\,t^2_{\text{Schwarzschild}}+\left(1-\frac{r_s}{r}\right)^{-1}\mathrm{d}\,r^2 \\ &\qquad\qquad =-\left(1-\frac{r_s}{r}\right)\mathrm{d}\,t^2+\left(1+\frac{r_s}{r}\right)\mathrm{d}\,r^2+2\frac{r_s}{r}\,\mathrm{d}\,t\,\mathrm{d}\,r \end{aligned}$$

under the transformation

$$t_{\text{Schwarzschild}}=t-r_s\ln\left|\frac{r}{r_s}-1\right|.$$

Substituting

$$\mathrm{d}\,t_{\text{Schwarzschild}}=\mathrm{d}\,t-\frac{1}{\frac{r_s}{r}-1}\,\mathrm{d}\,r$$

it follows

$$\begin{aligned} (\text{LHS}) &= -\left(1-\frac{r_s}{r}\right)\mathrm{d}\,t^2+\left(\frac{1}{1-\frac{r_s}{r}}-\frac{1-\frac{r_s}{r}}{\left(\frac{r}{r_s}-1\right)^2}\right)\mathrm{d}\,r^2+2\frac{1-\frac{r_s}{r}}{\frac{r_s}{s}-1}\,\mathrm{d}\,t\,\mathrm{d}\,r \\ &= -\left(1-\frac{r_s}{r}\right)\mathrm{d}\,t^2+\left(\frac{r}{r-r_s}-\frac{r_s^2(r-r_s)}{r(r-r_s)^2}\right)\mathrm{d}\,r^2+2\frac{r_s(r-r_s)}{r(r-r_s)}\,\mathrm{d}\,t\,\mathrm{d}\,r \\ &= -\left(1-\frac{r_s}{r}\right)\mathrm{d}\,t^2+\frac{(r+r_s)(r-r_s)}{r(r-r_s)}\,\mathrm{d}\,r^2+2\frac{r_s}{r}\,\mathrm{d}\,t\,\mathrm{d}\,r \\ &= (\text{RHS}) \end{aligned}$$

A.4 Christoffel Symbols of the Kerr-de Sitter Metric

There are 36 non-zero independent Christoffel symbols. As an example, the first, the longest and the shortest have been rendered, with term order as produced by *SageMath*:

$$\begin{aligned}\Gamma^t_{tt} = -\frac{1}{2}(a^2\chi^2\lambda+1)(2(a^4\chi^4+2a^2\chi^2r^2+r^4)(a^2\lambda+1)\lambda r \\ +(a^2\chi^2\lambda+1)(a^2\chi^2-r^2)r_s)rr_s\Big/ \\ \Big(a^{10}\chi^6\lambda^2+2a^8\chi^6\lambda+a^6\chi^6-(a^4\lambda^3+2a^2\lambda^2+\lambda)r^8 \\ -(3a^6\chi^2\lambda^3+(6a^4\chi^2-a^4)\lambda^2+(3a^2\chi^2-2a^2)\lambda-1)r^6 \\ -3(a^8\chi^4\lambda^3-a^2\chi^2+(2a^6\chi^4-a^6\chi^2)\lambda^2+(a^4\chi^4-2a^4\chi^2)\lambda)r^4 \\ -(a^{10}\chi^6\lambda^3-3a^4\chi^4+(2a^8\chi^6-3a^8\chi^4)\lambda^2+(a^6\chi^6-6a^6\chi^4)\lambda)r^2\Big)\end{aligned}$$

$$\begin{aligned}\Gamma^t_{tr} = \Gamma^t_{rt} = \frac{1}{2}\Big(2(a^2\lambda^3+\lambda^2)r^9+2(2a^2\chi^2\lambda^2+(2a^4\chi^2+a^4)\lambda^3-\lambda)r^7 \\ +2((a^6\chi^4+2a^6\chi^2)\lambda^3+(a^4\chi^4-a^4)\lambda^2-(2a^2\chi^2+a^2)\lambda)r^5 \\ +2(a^8\chi^4\lambda^3-2a^6\chi^2\lambda^2-(a^4\chi^4+2a^4\chi^2)\lambda)r^3 \\ +((a^2\chi^2\lambda+1)r^3-(a^4\chi^4\lambda+a^2\chi^2)r)r_s^2-2(a^8\chi^4\lambda^2+a^6\chi^4\lambda)r \\ -(a^6\chi^4\lambda+3(a^2\chi^2\lambda^2+\lambda)r^6+a^4\chi^2+(3a^2\lambda+(a^4\chi^4+3a^4\chi^2)\lambda^2-1)r^4 \\ +(a^6\chi^4\lambda^2+a^4\chi^4\lambda+a^2\chi^2-a^2)r^2)r_s\Big)\Big/ \\ \Big(a^8\chi^4\lambda+(a^2\lambda^3+\lambda^2)r^{10}+a^6\chi^4+((2a^4\chi^2+a^4)\lambda^3+(2a^2\chi^2-a^2)\lambda^2-2\lambda)r^8 \\ +((a^6\chi^4+2a^6\chi^2)\lambda^3+(a^4\chi^4-2a^4\chi^2-2a^4)\lambda^2-(4a^2\chi^2+a^2)\lambda+1)r^6 \\ +(a^8\chi^4\lambda^3+2a^2\chi^2-(a^6\chi^4+4a^6\chi^2)\lambda^2+a^2-(2a^4\chi^4+2a^4\chi^2-a^4)\lambda)r^4 \\ -(2a^8\chi^4\lambda^2-a^4\chi^4-2a^4\chi^2+(a^6\chi^4-2a^6\chi^2)\lambda)r^2\Big)\end{aligned}$$

$$\Gamma^\chi_{r\chi} = \Gamma^\chi_{\chi r} = r/(a^2\chi^2+r^2)$$

B Bibliography

[1] Michel A. Cuendet and Wilfred F. van Gunsteren. On the calculation of velocity-dependent properties in molecular dynamics simulations using the leapfrog integration algorithm. *The Journal of Chemical Physics*, 127(18):184102, 2007.

[2] Tekin Dereli and Metin Gürses. The generalized Kerr-Schild transform in eleven-dimensional supergravity. 171:209–211, 04 1986.

[3] R. D'Inverno. *Introducing Einstein's Relativity*. Clarendon Press, 1992.

[4] A. Einstein. Die Feldgleichungen der Gravitation. *Sitzungsberichte der Königlich Preußischen Akademie der Wissenschaften (Berlin), Seite 844-847.*, 1915.

[5] G.W. Gibbons, H. Lü, Don N. Page, and C.N. Pope. The general kerr–de sitter metrics in all dimensions. *Journal of Geometry and Physics*, 53(1):49 – 73, 2005.

[6] J. B. Griffiths and J. Podolsky. A New look at the Plebanski-Demianski family of solutions. *Int. J. Mod. Phys.*, D15:335–370, 2006.

[7] Metin Gürses and Feza Gürsey. Lorentz Covariant Treatment of the Kerr-Schild Metric. *J. Math. Phys.*, 16:2385, 1975.

[8] David Hilbert. Grundlagen der Physik, Erste Mitteilung. *Nachrichten von der Koeniglichen Gesellschaft der Wissenschaften zu Goettingen, Math-physik. Klasse*, 1915:395–407, 1915.

[9] R.P. Kerr and A. Schild. A new class of vacuum solutions of the Einstein field equations. *Atti del convegno sulla relatività generale; problemi dell'energia e ondi gravitationali*, pages 222–233, 1965.

[10] R.P. Kerr and A. Schild. Some algebraically degenerate solutions of Einstein's gravitational field equations. *Proc. Symp. Appl. Math 17*, page 199, 1965.

[11] Ivan Kolár, Jan Slovák, and Peter W Michor. *Natural operations in differential geometry*. 1999.

[12] Charles W. Misner, Kip S. Thorne, and John A. Wheeler. *Gravitation*. Physics Series. W. H. Freeman, San Francisco, first edition edition, September 1973.

[13] Thomas Mueller and Frank Grave. Catalogue of spacetimes. *arXiv:0904.4184*, 2009.

[14] J.F Plebanski and M Demianski. Rotating, charged, and uniformly accelerating mass in general relativity. *Annals of Physics*, 98(1):98 – 127, 1976.

[15] Miguel Preto and Scott Tremaine. A class of symplectic integrators with adaptive time step for separable hamiltonian systems. *The Astronomical Journal*, 118(5):2532, 1999.

[16] F.R.S. Sir F. W. Dyson, F.R.S. A. S. Eddington, and Mr. C. Davidson. Ix. a determination of the deflection of light by the sun's gravitational field, from observations made at the total eclipse of may 29, 1919. *Philosophical Transactions of the Royal Society of London A: Mathematical, Physical and Engineering Sciences*, 220(571-581):291–333, 1920.

[17] William Stein and David Joyner. SAGE: System for algebra and geometry experimentation. *ACM SIGSAM Bulletin*, 39(2):61–64, 2005.

[18] Hans Stephani, D. Kramer, Malcolm A. H. MacCallum, Cornelius Hoenselaers, and Eduard Herlt. *Exact solutions of Einstein's field equations*. Cambridge Monographs on Mathematical Physics. Cambridge Univ. Press, Cambridge, 2003.

[19] The Sage Developers. SageMath, the Sage Mathematics Software System (Version 8.1), 2017. `http://www.sagemath.org`.

[20] A. Trautman. On the propagation of information by waves. *Recent developments in general relativity*, page 459–463, 1962.

[21] Matt Visser. The Kerr spacetime: A brief introduction. In *Kerr Fest: Black Holes in Astrophysics, General Relativity and Quantum Gravity Christchurch, New Zealand, August 26-28, 2004*, 2007.

C Acknowledgements

In memory of Dr. Peter Gärtner, father, guide and friend.
You are missed.

I would like to express my deep gratitude to Professor Dr. Ralf Schneider for his supervision, encouragement and useful critique, and to Professor Dr. Lutz Schweikhard for his willingness to support this thesis. It has not been an easy time, and I wish to take this opportunity to extend special thanks to my family, my friends and anyone else who has offered a kind word over the past months. The night has been long, but the dawn is sure to break.

D Declaration of Authorship

I, Christoph Gärtner, declare that the accompanying bachelor's thesis titled 'Photon Dynamics in Curved Spacetimes' and the work presented therein are my own. I confirm that besides those specified explicitly, I did not use any other relevant sources of help. All passages that have been taken in word or meaning from other work have been marked as borrowed by giving the source, including secondary literature.

Greifswald,